Nonlinear Dynamics and Neuroscience

Article DOI: 10.18500/0869-6632-003165

Application of phase dynamics modeling and recurrence methods to assess the characteristics of the relationship between physiological rhythms[1]

O. E. Dick

Pavlov Institute of Physiology of the Russian Academy of Science, St. Petersburg, Russia
E-mail: ✉dickviola@gmail.com

Received 26.10.2024, accepted 13.01.2025, available online 3.02.2025, published 30.05.2025

Abstract. The *purpose* of this work is to apply two methods of nonlinear dynamics to assess the characteristics of the relationship between time series extracted from physiological rhythms. The analyzed time series were respiratory rhythm fluctuations, arterial pressure variability curves, and variability of neuronal activity intervals in the medulla oblongata of rats before and during pain exposure. *Methods.* To solve the problem of identifying the relationship and assessing the asymmetry and direction of the relationship, a method for modeling the phase dynamics of weakly coupled and weakly noisy systems and a method for calculating averaged conditional probabilities of recurrences of time series generated by interacting systems were used. As characteristics of the relationship between systems, estimates of the intensity of the influence of one system on another and estimates in the differences of the averaged conditional probabilities of recurrences were used. *Results.* To verify the robustness of the applied methods to noise, an analysis of a well-studied model of unidirectionally coupled van der Pol oscillators was performed. The correct determination of the direction of coupling by both methods with weak noise and a decrease in the possibility of identifying the direction by the phase modeling method with increasing noise, and the preservation of the possibility of correctly determining the direction by the recurrence method were confirmed. For experimentally obtained and weakly noisy biological time series, an asymmetry of the coupling with a predominant influence of the respiratory rhythm on the variability of neuronal activity and arterial pressure, and the influence of arterial pressure variability on the neuronal activity of the reticular formation of the medulla oblongata was found in most of the analyzed data. *Conclusion.* The application of two methods for assessing the characteristics of the relationship between weakly noisy time series, both model and experimental, showed quite consistent results in the predominant influence of one system on the other.

Keywords: phase dynamics, recurrence, physiological rhythms.

Acknowledgements. The work was supported by the State funding allocated to the Pavlov Institute of Physiology Russian Academy of Sciences (No. 1021062411784-3-3.1.8).

For citation: Dick OE. Application of phase dynamics modeling and recurrence methods to assess the characteristics of the relationship between physiological rhythms. Izvestiya VUZ. Applied Nonlinear Dynamics. 2025;33(3): 381–398. DOI: 10.18500/0869-6632-003165

Introduction

The study of the characteristics of the relationship between weakly coupled dynamical systems is of considerable interest due to the fact that clarifying the direction of relationship is important for

[1]The paper presents materials of a talk given at the conference "Neuroinformatics — 2024"

understanding the mechanism of functioning of interacting systems. When analyzing biological systems such as the cardiovascular and respiratory systems, the predominant effect of low-frequency oscillations in heart rate variability on the variability of arterial vascular blood supply was determined in [1, 2] while a violation of heart rate causes a violation of the regulation of arterial vascular tone. In the works [3–6] the dominant influence of respiratory rhythm oscillations in relation to cardiovascular rhythm oscillations was determined. Breathing controls the phase synchronization between blood pressure and heart rate oscillations [7]. Pathological conditions can change the interactions of physiological systems, for example, as a result of a myocardial infarction, the duration of synchronization decreases [1, 8]. However, the relationship between the respiratory and nervous systems is considered to be not entirely clear [9], therefore, obtaining additional information about the direction of relationships in the systems under consideration seems to be a very urgent task. Various methods of nonlinear dynamics can be used to evaluate directional coupling [10, 11]. These are methods related to determining the Granger causality [12], transfer entropy [13], partial directed coherence [14], calculating the directivity index using phase dynamics modeling [5,15,16], determining joint recurrences and calculating the average conditional probabilities of recurrences between two phase trajectories of the analyzed [17,18]. These approaches have been recognized in various applications in the fields of physiology [3,19–23] and climatology [24,25].

The purpose of this work is to find the characteristics of the relationship (direction and intensity of influence of one system on another) between time series extracted from the physiological rhythms of various systems, by modeling the phase dynamics of weakly coupled and weak noise periodic processes and by calculating the average conditional recurrence probabilities.

The analyzed time series used fluctuations in respiratory rhythm (RES), curves of blood pressure variability (BPV) and variability of neuronal activity (NAV) of the rat medulla oblongata, obtained in [26] before and during pain exposure, which is a mechanical stretching of the colon using a rubber balloon. In [26] these data were used to identify phase synchronization between pairwise time series using a synchrosqueezed wavelet transform. In this work, these data are used to analyze the characteristics of the relationship between physiological rhythms and to determine their changes during pain exposure. The methods used are described in section 1. To test the stability of methods for analyzing the characteristics of the relationship between two time series to noise, a well-studied model of two unidirectionally coupled oscillators with known phase synchronization properties is considered in section 2.1. Section 2.2 presents the results of applying these methods to experimental data.

1. Methods

1.1. Determining the characteristics of coupling between interacting systems based on the analysis of joint recurrences. To analyze the coupling between weakly interacting systems by finding joint recurrences, it is first necessary to construct the phase trajectories x and y from the initial signals $X(t)$ and $Y(t)$, generated by the systems X and Y [27]. The time delay method is used for this purpose [28]:

$$x(t) = (X(t), X(t+d), ..., X(t+(m-1)d), \tag{1}$$

$$y(t) = (Y(t), Y(t+d), ..., Y(t+(m-1)d), \tag{2}$$

where d is the time delay and m is the embedding dimension, determined by the methods of searching for the minimum of the mutual information function [29] and the minimum of the nearest false neighbors [30], respectively. Then, for the constructed trajectories x and y, the recurrence matrices are calculated [27]:

$$R^X_{i,j} = \Theta(\varepsilon_X - ||x_i - x_j||), \tag{3}$$

$$R^Y_{i,j} = \Theta(\varepsilon_Y - ||y_i - y_j||), \tag{4}$$

where Θ is the Heaviside function, $N = n - (m-1)d$, n is the length of the analyzed signals $X(t)$ and $Y(t)$, $i, j = 1, ..., N$, ε_X and ε_Y are the radii of the neighborhoods of the points of the phase trajectories, the values of which are chosen so that the density of recurrent points $RR = \frac{1}{N^2}\sum_{i=1}^{N} RR_{i,j}$ for both recurrence matrices is the same [27]. The matrix of joint recurrences $JR^{X,Y}_{i,j}$ is calculated using the

equation [27]

$$JR_{i,j}^{X,Y} = \Theta(\varepsilon_X - ||x_i - x_j||)\Theta(\varepsilon_Y - ||y_i - y_j||). \tag{5}$$

The calculated matrices are used to determine the average conditional probabilities of recurrence (MCR) [17]:

$$\mathrm{MCR}(X|Y) = \frac{1}{N}\sum_{i=1}^{N}\frac{p(x_i, y_i)}{p(y_i)} = \frac{1}{N}\sum_{i=1}^{N}\frac{\sum_{j=1}^{N} JR_{i,j}^{X,Y}}{\sum_{j=1}^{N} R_{i,j}^{Y}}, \tag{6}$$

$$\mathrm{MCR}(Y|X) = \frac{1}{N}\sum_{i=1}^{N}\frac{p(x_i, y_i)}{p(x_i)} = \frac{1}{N}\sum_{i=1}^{N}\frac{\sum_{j=1}^{N} JR_{i,j}^{X,Y}}{\sum_{j=1}^{N} R_{i,j}^{X}}. \tag{7}$$

Meeting the condition $\triangle\mathrm{MCR}(X|Y) = 0$ for interacting systems means that there is a symmetry of coupling, and meeting the condition $\triangle\mathrm{MCR}(X|Y) = \mathrm{MCR}(X|Y) - \mathrm{MCR}(Y|X) > 0$ means an asymmetry of the coupling with the direction in which the system X has a greater influence on the system Y, that is, the system X controls system Y [17, 18]. Thus, this method allows you to determine the direction of coupling of interacting systems in the presence of asymmetry of the coupling using the coupling asymmetry index $\triangle\mathrm{MCR}(X|Y)$. The advantages of the method of estimating the characteristics of directional coupling using joint recurrence relations are the possibility of its use for noise and rather short time series, which is relevant for the analysis of experimental biological records [31].

1.2. Determination of the characteristics of the relationship between interacting systems by the method of modeling phase dynamics. The method of modeling phase dynamics involves the construction of an experimental model of the phase dynamics of the analyzed systems based on time series representing the signals of the systems. For these signals, the instantaneous phases $\phi_X(t)$ and $\phi_Y(t)$, are calculated, and then a model of phase dynamics is constructed with phase increments over the time interval τ:

$$\phi_X(t+\tau) - \phi_X(t) = F_X(\phi_X(t), \phi_Y(t), a_X) + \varepsilon_X(t), \tag{8}$$

$$\phi_Y(t+\tau) - \phi_Y(t) = F_Y(\phi_X(t), \phi_Y(t), a_Y) + \varepsilon_Y(t), \tag{9}$$

where $\varepsilon_X(t)$ and $\varepsilon_Y(t)$ are Gaussian noises with zero mean. Functions $F_X(\phi_X(t), \phi_Y(t), a_X) + \varepsilon_X(t)$ and $F_Y(\phi_X(t), \phi_Y(t), a_Y) + \varepsilon_Y(t)$ are described by polynomials of the form [5, 32]:

$$F_j(\phi_X, \phi_Y, a_j) = \sum_{m,n} a_{j,m,n} \exp(i(m\phi_X + n\phi_Y), \quad j = X, Y. \tag{10}$$

According to [5, 32], the values of τ are equal to the smaller of the characteristic oscillation periods for the two analyzed signals, and $m < 4$, $n < 4$. To estimate the values of the coefficients $a_{j,m,n}$ the minimum of the objective function is found

$$S_j^2 = \sum_{i=1}^{N-\tau}(\triangle\phi_j(t_i) - F_j(\phi_X(t_i), \phi_Y(t_i), a_j))^2, \quad j = X, Y \tag{11}$$

using the least squares method.

Based on the calculated functions $F_j(\phi_X(t), \phi_Y(t), a_j)$, $j = X, Y$ the quantitative characteristics of the directional coupling of interacting systems are determined as the intensity of the influence of one system on another. The intensity of the impact of the system Y on the system X is defined as the steepness of the dependence of the function F_X on ϕ_Y, and the influence of the system X on the system Y is defined as the steepness of the dependence of the function F_Y on ϕ_X [5]:

$$c_X^2 = \frac{1}{2\pi^2}\int_0^{2\pi}\int_0^{2\pi}\left(\frac{\partial F_X(\phi_X, \phi_Y, a_X)}{\partial\phi_Y}\right)^2 d\phi_X d\phi_Y, \tag{12}$$

$$c_Y^2 = \frac{1}{2\pi^2}\int_0^{2\pi}\int_0^{2\pi}\left(\frac{\partial F_Y(\phi_X, \phi_Y, a_Y)}{\partial\phi_X}\right)^2 d\phi_X d\phi_Y. \tag{13}$$

In this regard, the value of c_X is a quantitative characteristic of the directional coupling $Y \to X$, and c_Y is a quantitative characteristic of the directional coupling $X \to Y$.

For short time series (with a length of 50 characteristic periods typical of real signals), the work [32] proposed unbiased estimates of the values c_X^2 and c_Y^2, used in this work, calculated according to the formulas, given in [32]:

$$\gamma_j = c_j^2 - r_j = c_j^2 - \sum_k n_k^2 \sigma_{j,k}^2, \quad j = X, Y, \tag{14}$$

where r_X and r_Y are corrections depending on the noise level and the length of the time series, $k = 1, ..., L$, where L is the number of coefficients of the polynomials $F_X(\phi_X, \phi_Y, a_X)$ and $F_Y(\phi_Y, \phi_X, a_Y)$. The values of unbiased dispersion estimates $\sigma_{X,k}^2$ and $\sigma_{Y,k}^2$ of coefficients $a_{X,k}$ and $a_{Y,k}$ of function polynomials $F_X(\phi_X, \phi_Y, a_X)$ and $F_Y(\phi_Y, \phi_X, a_Y)$ are calculated using the formulas of work [32], given in the Appendix. These corrections provide zero bias (zero systematic error) and possible negative values of γ_X and γ_Y [32, 33]. However, negative values indicate that the unbiased estimates are not significantly different from zero [32, 33]. Finding estimates of the dispersion of $\sigma_{\gamma_X}^2$ and $\sigma_{\gamma_Y}^2$ for the values of γ_X and γ_Y using the formulas in the Appendix allows you to determine 95 percent confidence intervals $[\gamma_X - 1.6\sigma_{\gamma_X}, \gamma_X + 1.8\sigma_{\gamma_X}]$ and $[\gamma_Y - 1.6\sigma_{\gamma_Y}, \gamma_Y + 1.8\sigma_{\gamma_Y}]$ [32] (here, for convenience, we denote $\sigma_X = \sigma_{\gamma_X}$ and $\sigma_X = \sigma_{\gamma_X}$).

When conditions $\gamma_X - 1.6\sigma_X > 0$ are met, it is concluded that system Y influences system X with an error probability of no more than 0.05, and when condition $\gamma_Y - 1.6\sigma_Y > 0$ is met, the predominant influence of system X on system Y is taken into account with the same error probability [32, 34]. If both conditions are fulfilled simultaneously, it is concluded that the two systems have a mutual influence on each other.

Due to the fact that the direction of coupling can only be determined for experimental data for which the value of the phase synchronization index ρ does not exceed the value of 0.6 [32], the phase synchronization index was pre-calculated [3]

$$\rho = \left| \frac{1}{N} \sum_{j=1}^{N} \exp(2\pi i(\phi_X(t + j\triangle t/N) - \phi_Y(t + j\triangle t/N)) \right| \tag{15}$$

in a sliding window with a width of $\triangle t$ and a sliding window offset equal to the sampling interval.

The instantaneous phases $\phi_X(t)$ and $\phi_Y(t)$ were calculated using the synchrosqueezed wavelet transform [35], described in detail in our previous work [26] based on finding the ridges (frequency components of the signal) by solving the conditional optimization of the search among all curves for those that maximize the coefficients of the synchrosqueezed wavelet transform.

To assess the statistical significance of the calculated values of the phase synchronization index ρ and the coupling asymmetry index $\triangle$MCR, a statistical test was applied with the creation of surrogate time series based on recurrences [36]. The null hypothesis was that the signalsы $X(t)$ and $Y(t)$ have independent recurrent structures. The statistical test included calculating 100 surrogates $Y_{\text{surr}j}$ and $X_{\text{surr}j}$, $j = 1, ..., 100$, calculating synchronization indicators ρ and coupling asymmetry $\triangle$MCR (we denote them in general, $A_{\text{surr}j}$) for each surrogate and getting the distribution of values A_{surr}, and then finding statistics

$$Z = \left| \frac{A - \overline{A_{\text{surr}}}}{\sigma_{\text{surr}}} \right|, \tag{16}$$

where $\overline{A_{\text{surr}}}$ is the average and σ_{surr} is the standard deviation. The null hypothesis was rejected at 95% significance level in the case of $Z > 1.96$, and the value of (synchronization index ρ or coupling asymmetry $\triangle$MCR) was considered statistically significant [36].

2. Results

2.1. Application of methods for finding directional coupling characteristics for the van der Pol oscillator model. Two unidirectionally coupled systems of X and Y van der Pol oscillators were considered as a model:

$$\frac{d^2x}{dt^2} = 0.5(1-x^2)\frac{dx}{dt} - \omega_X^2 x + \xi_1(t), \tag{17}$$

$$\frac{d^2y}{dt^2} = 0.5(1-y^2)\frac{dy}{dt} - \omega_Y^2 y + \mu(\frac{dx}{dt} - \frac{dy}{dt}) + \xi_2(t) \tag{18}$$

with frequencies $\omega_X = 1.11$ and $\omega_Y = 0.89$, the coupling parameter μ and the noise components $\xi_X(t)$ and $\xi_Y(t)$ in the form of Gaussian white noise with zero mean and an autocovariation function $\langle \xi_X(t)\xi_X(t')\rangle = D\delta(t-t')$, where $\delta(t-t')$ is the Dirac delta function and D is the intensity noise.

Equations (17)–(18) were integrated with a step of 0.03 s and an integration time of 600 s, which corresponded to 20000 points.

Fig. 1 illustrates the influence of noise level on oscillator oscillations, phase synchronization indicators ρ and coupling directions γ_1, γ_2 and $\triangle\mathrm{MCR}(X|Y)$ for two unidirectionally coupled systems. The phase variables x and y and the trajectories of the oscillators X and Y are constructed for the coupling parameter $\mu = 0.15$ at two noise levels $D = 0.1$ (Fig. 1, *a*–*c*) and $D = 0.7$ (Fig. 1, *d*–*f*). The time realizations obtained at different noise levels show that an increase in noise intensity distorts oscillator oscillations to a greater extent, increasing the spread of random trajectories around periodic trajectories corresponding to the absence of noise.

To calculate the values of $\triangle\mathrm{MCR}(X|Y)$ the time delay parameters $d = 10$ and the embedding dimension $m = 7$ were determined by searching for the minimum of the mutual information function [30] and the minimum of the nearest false neighbors [29] respectively. The threshold values ε_X and ε_Y were chosen so as to have a fixed recurrence density of $RR = 0.1$ in both recurrence matrices for system X and system Y [17, 18].

For each value of the coupling strength μ in the range from 0.05 to 0.21, the average values for 100 trajectories for uniformly distributed initial conditions and their corresponding standard deviations for ρ and $\triangle\mathrm{MCR}(X|Y)$ were calculated. For estimates of the indicators of the direction of coupling γ_X and γ_Y confidence intervals are constructed using the formulas (19)–(23) in the Application. Curves $\rho(\mu)$, $\gamma_X(\mu)$ and $\gamma_Y(\mu)$, and $\triangle\mathrm{MCR}(X|Y)(\mu)$ are constructed for two noise levels (noise intensity $D = 0.3$ corresponds to curves with round points and $D = 0.7$ corresponds to curves with square points). As the coupling strength increases, the value of the phase synchronization index increases more with a lower noise level (Fig. 1, *g*). For $\mu = 0.21$ $\rho = 0.65 \pm 0.09$ at noise intensity $D = 0.3$ and $\rho = 0.89 \pm 0.12$ at a noise level of $D = 0.7$.

The method of modeling phase dynamics allows us to reliably determine the direction of coupling of two unidirectionally coupled systems in the model under consideration only with a coupling strength of $\mu \leqslant 0.19$ at a noise level of $D = 0.3$ and with a coupling strength of $\mu \leqslant 0.17$ and a noise level of $D = 0.7$ due to the fact that at high values of the coupling strength, the value of the phase synchronization index exceeds the threshold value of $\rho_{\mathrm{crit}} = 0.6$ [32]. For $\rho < \rho_{\mathrm{crit}}$ the values of the coupling direction characteristics satisfy the conditions $\gamma_X \pm 1.6\sigma_X < 0$ (Fig. 1, *h*) and $\gamma_Y \pm 1.6\sigma_{Y2} > 0$ (Fig. 1, *i*), which corresponds to the known effect of system X on system Y with an error probability of no more than 0.05 [32, 34].

In contrast, the method of detecting coupling asymmetry between interacting systems based on the analysis of joint recurrences allows us to determine the direction of coupling in this

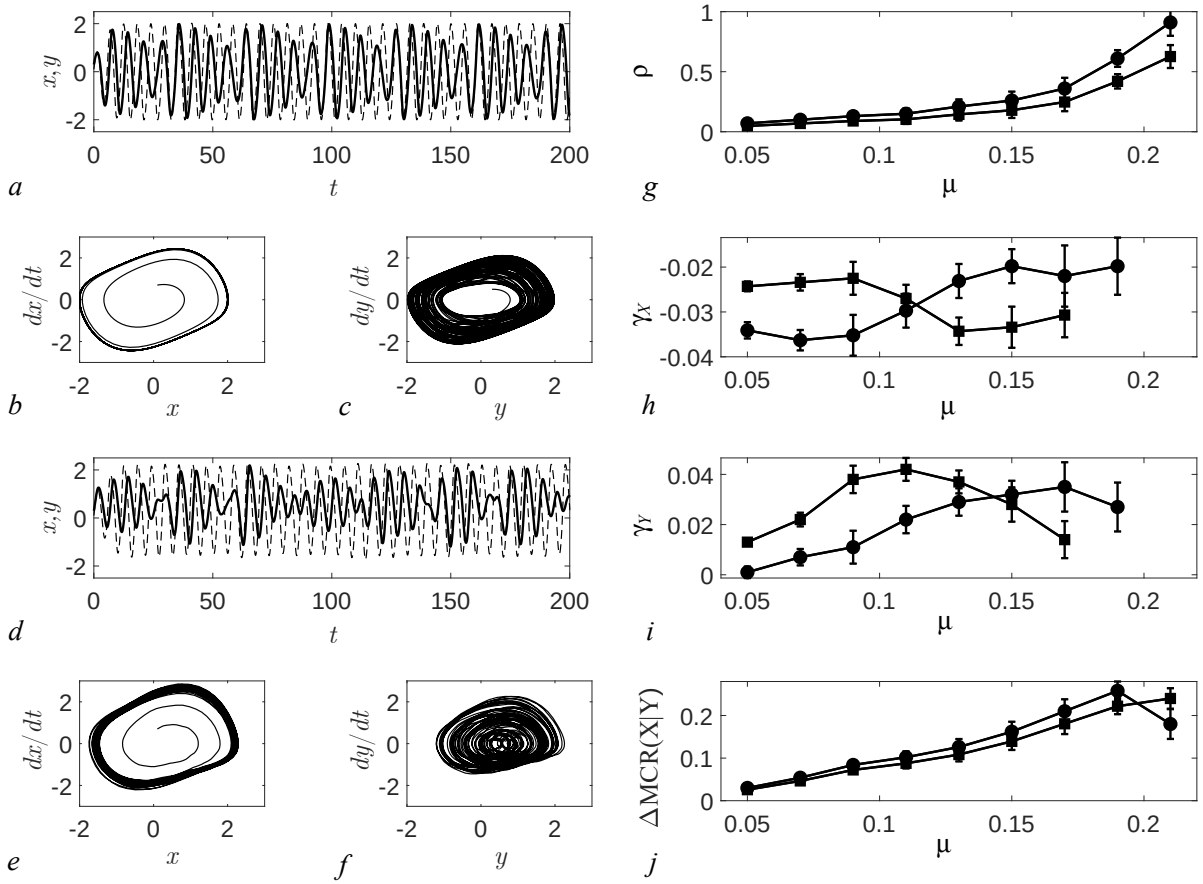

Fig. 1. Phase variables x and y at $D = 0.1$ (a) and $D = 0.7$ (d) and trajectories of oscillators X and Y at $D = 0.1$ (b, c) and $D = 0.7$ (e, f) for the coupling parameter $\mu = 0.15$. Dependencies of values of the index phase synchronization and coupling directionality indices from the coupling parameter μ for the model of unidirectionally coupled van der Pol generator systems: $\rho(\mu)$ (g); $\gamma_X(\mu)$ (h); $\gamma_Y(\mu)$ (i); $\triangle\mathrm{MCR}(X|Y)(\mu)$ (j). Curves with round points are plotted for noise intensity $D = 0.3$, curves with square points are plotted for $D = 0.7$

model of unidirectionally coupled van der Pol generators for all analyzed values of the coupling parameter $0.05 \leqslant \mu \leqslant 0.21$. For all these values of μ the coupling asymmetry indicators satisfy the condition $\triangle\mathrm{MCR}(X|Y) > 0$ with a noise intensity of $D = 0.3$ and $D = 0.7$ (Fig. 1, j), that is, the asymmetry of the coupling between the system X and the system Y is preserved, and the system X is the master, and the system Y remains the slave when the noise level increases and when phase synchronization is reached. The indication that the indicators of coupling asymmetry based on the analysis of recurrences correctly determine the direction of coupling before and during phase synchronization is consistent with the results of [17,39], which show that the onset of phase synchronization for the model of two non-identical unidirectionally coupled Lorentz systems does not change the coupling asymmetry. Generalized synchronization leads to the disappearance of coupling asymmetry, leading $\triangle\mathrm{MCR}(X|Y) = 0$ [39].

It is known that as the noise level increases, it becomes more difficult to detect coupling asymmetry for very small values of coupling strength, since the values of $\mathrm{MCR}(X|Y)$ and $\mathrm{MCR}(Y|X)$ are almost the same, so the higher the noise level, the stronger the coupling strength must be to detect the asymmetry [17]. However, even at relatively high noise levels, coupling asymmetry can still be correctly detected for relatively small coupling strengths using the recurrence method [17].

2.2. Application of methods for finding characteristics of the coupling between physiological rhythms. The physiological data used for the analysis are described in detail and shown in Fig. 1 in the article [26]. These are simultaneously recorded oscillations of blood pressure, respiration, and neuronal activity of the reticular formation of the medulla oblongata for 10 rats with a recording length of 60 seconds before and 60 seconds during pain exposure with a sampling frequency of 10000 Hz and a repetition of 5 times after 60 seconds of relaxation.

In this work, 30 pairs of unartifact time series were analyzed, representing oscillations of respiratory rhythm (RES), isolated curves of variability of neuronal activity intervals (NAV) and curves of blood pressure variability intervals (BPV). These curves contained sequences of time intervals between local maxima of the initial data of neuronal activity and blood pressure. The obtained curves were approximated by cubic splines with oversampling to a frequency of 1000 Hz and removal of nonlinear trends.

Bandpass filtering of BPV and NAV time series, removing frequencies less than 1 Hz and more than 2.5 Hz, was used to isolate the components of variability in the intervals of neuronal activity and blood pressure with basic frequencies close to the respiratory rhythm frequency. When determining the values of the coupling direction indicators, we used pairs of normalized time series to have a zero mean and a single standard deviation.

To calculate the values of $\triangle$MCR we used the values of the embedding dimension m and the delay d, determined by the methods of searching for the minimum of the nearest false neighbors [29] and the minimum of the mutual information function [30] respectively. First, the optimal parameters m and d were determined for each time series NAV, BPV, RES. The values $m_1 > m_2 > m_3$, $d_3 > d_2 > d_1$ were obtained for all 30 rows. On average, these values are $m_1 = 5$, $d = 15$ for NAV, $m_2 = 4$, $d_2 = 17$ for BPV, $m_3 = 3$, $d_3 = 20$ for RES.

The recurrence matrices, according to the formulas (3), (4), were calculated for the specified values m_1, m_2, m_3, d_1, d_2, d_3, and the joint recurrence matrices, in accordance with the formula (5), were calculated for the values $m = \max m_1, m_2, m_3 = 5$ and $d = \min d_1, d_2, d_3 = 15$.

The thresholds ε_X and ε_Y were selected $\varepsilon_X = \varepsilon_Y = \varepsilon = 0.05$. For verification, we applied calculations for various values of ε in the range from 0.01 to 0.3 and for various values of m in the range from 3 to 5 and found that the results of calculating $\triangle$MCR are insensitive to the choice of these values.

In Fig. 2 provides examples of calculating the phase difference between the NAV and BPV time series ($\triangle\phi_{\text{NAV}-\text{BPV}}$) (Fig. 2, *a*), the BPV and RES time series ($\triangle\phi_{\text{BPV}-\text{RES}}$) (Fig. 2, *b*) and the coupling function $F_{\text{BPV}}(\phi_{\text{NAV}}, \phi_{\text{BPV}})/\tau$, $F_{\text{NAV}}(\phi_{\text{NAV}}, \phi_{\text{BPV}})/\tau$, $F_{\text{RES}}(\phi_{\text{RES}}, \phi_{\text{BPV}})/\tau$, $F_{\text{BPV}}(\phi_{\text{BPV}}, \phi_{\text{RES}})/\tau$ (Fig. 2, *c–f*), the values of which are divided by $\tau = 0.5$ (c), equal to the smaller of the characteristic oscillation periods for the two analyzed signals.

Fig. 2, *e, f* illustrate a variant of the relationship between respiratory oscillations and blood pressure variability intervals. Function $F_{\text{BPV}}(\phi_{\text{BPV}}, \phi_{\text{RES}})/\tau$ it is characterized by a large range of changes in values (Fig. 2, *f*) compared to the function $F_{\text{RES}}(\phi_{\text{BPV}}, \phi_{\text{RES}})/\tau$, fluctuating around the circular frequency $\omega = 2\pi f_{\text{BPV}} \approx 12.1$ (Fig. 2, *e*). The other pair of time series NAV and BPV is characterized by a smaller range of fluctuations in the coupling function $F_{\text{BPV}}(\phi_{\text{BPV}}, \phi_{\text{NAV}})/\tau$ around the circular frequency $\omega = 2\pi f_{\text{BPV}} \approx 12.5$ (Fig. 2, *c*) compared to function $F_{\text{NAV}}(\phi_{\text{BPV}}, \phi_{\text{NAV}})/\tau$ (Fig. 2, *d*).

The values of the phase synchronization indices between the variability of neuronal activity and the blood pressure variability, as well as for synchronization between the blood pressure variability and the rhythm of breathing in these examples are less than the critical value of 0.6 ($\rho_{\text{BPV}-\text{NAV}} = 0.24$, $\rho_{\text{RES}-\text{BPV}} = 0.27$), which allows us to determine the characteristics of the coupling between the analyzed time series.

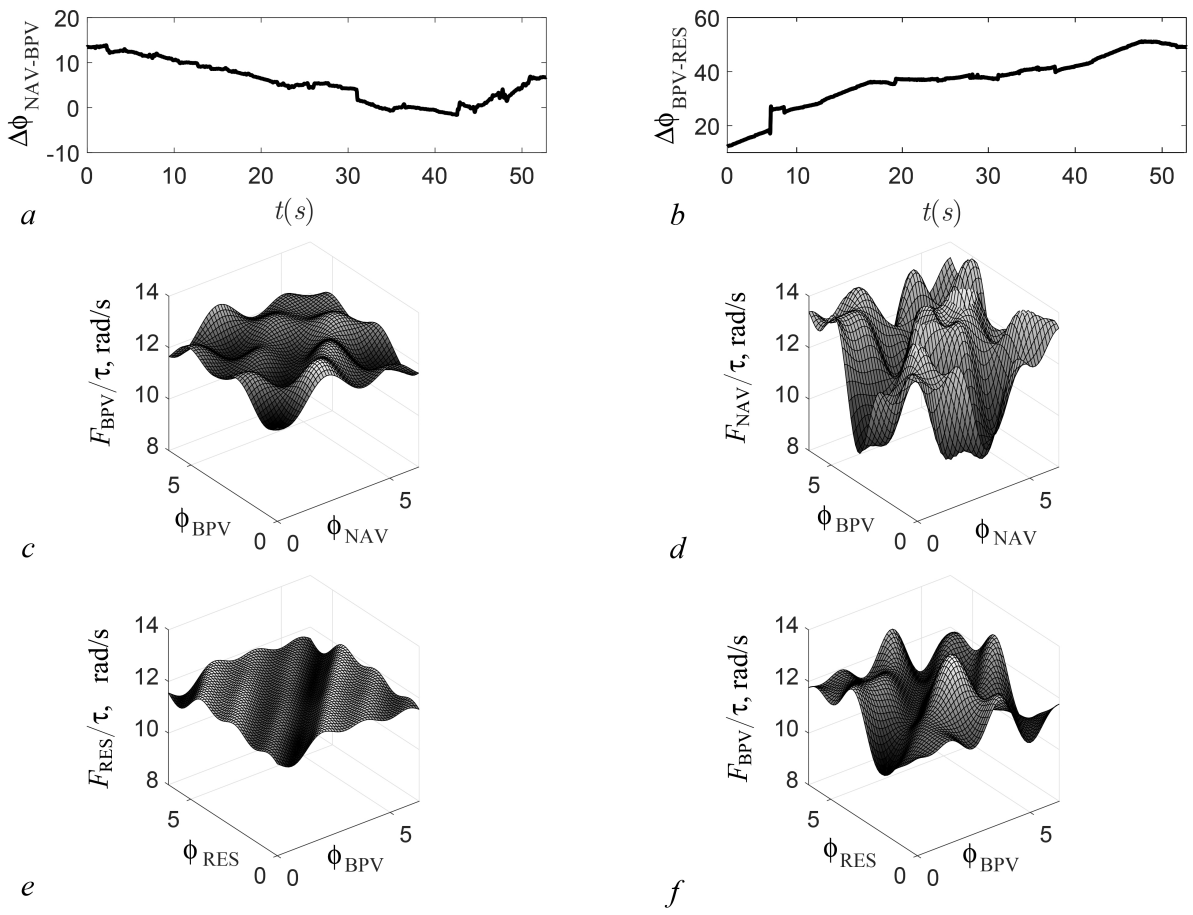

Fig. 2. Examples of calculating the phase difference of time series NAV and BPV and time series BPV and RES and the coupling functions. a — $\triangle\phi_{\mathrm{NAV-BPV}}$; b — $\triangle\phi_{\mathrm{BPV-RES}}$; c — $F_{\mathrm{BPV}}(\phi_{\mathrm{NAV}},\phi_{\mathrm{BPV}})/\tau$; d — $F_{\mathrm{NAV}}(\phi_{\mathrm{NAV}},\phi_{\mathrm{BPV}})/\tau$; e — $F_{\mathrm{RES}}(\phi_{\mathrm{BPV}},\phi_{\mathrm{RES}})/\tau$; f — $F_{\mathrm{BPV}}(\phi_{\mathrm{BPV}},\phi_{\mathrm{RES}})/\tau$

Estimates of $\gamma_{\mathrm{NAV}} - 1.6\sigma_{\mathrm{NAV}} = 0.13$ and $\gamma_{\mathrm{BPV}} - 1.6\sigma_{\mathrm{BPV}} = -0.08$ for one pair of time series indicate the influence of the cardiovascular system nervous, while the estimates of $\gamma_{\mathrm{BPV}} - 1.6\sigma_{\mathrm{BPV}} = 0.19$ and $\gamma_{\mathrm{RES}} - 1.6\sigma_{\mathrm{RES}} = -0.09$ for another pair of time series, it can be concluded that the respiratory rhythm has a significant influence on the blood pressure variability intervals in this example.

Before the pain exposure, phase synchronization was absent in 100% of the analyzed time series between fluctuations in respiratory rhythm and blood pressure variability, between variability of neuronal activity and blood pressure variability, as well as between respiratory rhythm and neuronal activity variability. The average values of the phase synchronization index satisfied the condition $\rho < 0.06$ and were, respectively, equal to $\rho_{\mathrm{BPV-NAV}} = 0.23 \pm 0.06$, $\rho_{\mathrm{RES-BPV}} = 0.31 \pm 0.07$, $\rho_{\mathrm{NAV-RES}} = 0.19 \pm 0.05$.

Pain exposure led to phase synchronization between the NAV and BPV time series in 43% of the data (13 out of 30), in 36% (11 out of 30) between the RES and BPV time series, and in 33% (10 out of 30) between the NAV and RES time series. The values of the phase synchronization index for these data satisfied the condition $\rho > 0.06$ and were equal to $\rho_{\mathrm{BPV-NAV}} = 0.78 \pm 0.12$, $\rho_{\mathrm{RES-BPV}} = 0.81 \pm 0.14$, $\rho_{\mathrm{NAV-RES}} = 0.76 \pm 0.11$.

In this regard, the direction of coupling was determined only for time series for which there

Table. Averaged coupling characteristics △MCR(BPV|NAV), △MCR(RES|BPV), △MCR(NAV|RES), $\gamma_{NAV} - 1.6\sigma_{NAV}$, $\gamma_{BPV} - 1.6\sigma_{BPV}$, $\gamma_{RES} - 1.6\sigma_{RES}$ before and during pain exposure

	before exposure	**before exposure**	**during exposure**	**during exposure**
	BPV→NAV	BPV – NAV	BPV→NAV	BPV – NAV
△MCR(BPV|NAV)	0.12 ± 0.03	0.03 ± 0.01	0.17 ± 0.04	0.05 ± 0.02
$\gamma_{NAV} - 1.6\sigma_{NAV}$	0.11 ± 0.03	0.08 ± 0.02	0.15 ± 0.04	0.07 ± 0.02
$\gamma_{BPV} - 1.6\sigma_{BPV}$	< 0	0.07 ± 0.02	< 0	0.08 ± 0.02
	RES→BPV	RES – BPV	RES→BPV	RES – BPV
△MCR(RES|BPV)	0.16 ± 0.04	0.04 ± 0.01	0.21 ± 0.04	0.06 ± 0.02
$\gamma_{BPV} - 1.6\sigma_{BPV}$	0.17 ± 0.05	0.09 ± 0.02	0.13 ± 0.03	0.12 ± 0.03
$\gamma_{RES} - 1.6\sigma_{RES}$	< 0	0.06 ± 0.02	< 0	0.13 ± 0.04
	RES→NAV	RES – NAV	RES→NAV	RES – NAV
△MCR(NAV|RES)	-0.18 ± 0.05	0.05 ± 0.01	-0.13 ± 0.04	0.03 ± 0.01
$\gamma_{RES} - 1.6\sigma_{RES}$	< 0	0.12 ± 0.03	< 0	0.09 ± 0.02
$\gamma_{NAV} - 1.6\sigma_{NAV}$	0.16 ± 0.05	0.13 ± 0.03	0.21 ± 0.06	0.11 ± 0.03

was no phase synchronization and the synchronization index satisfied the condition $\rho < 0.6$. The average values of the phase synchronization index in this case are respectively $\rho_{BPV-NAV} = 0.18 \pm 0.03$ for 57% of the data (17 out of 30), $\rho_{RES-BPV} = 0.22 \pm 0.05$ for 64% of the data (19 of 30) and $\rho_{NAV-RES} = 0.26 \pm 0.06$ for 67% of the data (20 of 30).

The table shows the average coupling characteristics △MCR(BPV|NAV), △MCR(RES|BPV), △MCR(NAV|RES), $\gamma_{NAV} - 1.6\sigma_{NAV}$, $\gamma_{BPV} - 1.6\sigma_{BPV}$, $\gamma_{RES} - 1.6\sigma_{RES}$ before and during pain exposure.

These averages were calculated for 28 pairs of time series before exposure and 16 pairs of time series during exposure, for which the condition $\rho < 0.6$ was met and for which statistically significant values of the coupling asymmetry index △MCR obtained after applying a statistical test with the creation of surrogate time series.

The error estimate in the Table for △MCR corresponds to the standard deviation for the analyzed time series, and the error estimates for the data using the phase modeling method correspond to the average values of the estimates σ_{NAV}, σ_{BPV}, σ_{RES}, obtained using formulas from [33], specified in the Appendix.

The asymmetry of the coupling before pain exposure was revealed between the NAV and BPV time series for 77% of the data (22 out of 28) using the analysis of joint recurrences. The average value of the coupling asymmetry index $\triangle MCR(BPV|NAV) = 0.12 \pm 0.03$ indicates the predominant influence of blood pressure variability on the variability of neuronal activity in these data.

Using phase dynamics modeling, estimates $\gamma_{NAV} - 1.6\sigma_{NAV} = 0.11 \pm 0.03$ and $\gamma_{BPV} - 1.6\sigma_{BPV} = -0.06 \pm 0.02$ were obtained for 72% data (20 out of 28) of the NAV and BPV, which also indicate a unidirectional influence of blood pressure variability on the variability of neuronal activity in these data with an error probability of no more than 0.05.

For the other analyzed data, the coupling between the NAV and BPV time series was determined to be symmetric. This is due to the fact that the differences in indicators MCR(NAV|BPV) and MCR(BPV|NAV) are insignificant and the value of the coupling asymmetry indicator is close

to zero: $\triangle$MCR(BPV|NAV) $= 0.03 \pm 0.01$, and both estimates of coupling direction indicators are positive: $\gamma_{\mathrm{NAV}} - 1.6\sigma_{\mathrm{NAV}} = 0.08 \pm 0.02$, $\gamma_{\mathrm{BPV}} - 1.6\sigma_{\mathrm{BPV}} = 0.07 \pm 0.02$. Thus, the results of using both methods allow us to conclude that the rhythms of the nervous and cardiovascular systems are interdependent in no more than 23% of the analyzed data.

The unidirectional coupling before pain exposure was also determined between the RES and BPV time series for 76% of the data (21 out of 28) using joint recurrence analysis (average value of the coupling asymmetry index $\triangle$MCR(RES|BPV) $= 0.16 \pm 0.04$) and for 72% of the data (20 out of 28) using phase dynamics modeling (estimates of coupling indicators $\gamma_{\mathrm{BPV}} - 1.6\sigma_{\mathrm{BPV}} = 0.17 \pm 0.05$, $\gamma_{\mathrm{RES}} - 1.6\sigma_{\mathrm{RES}} = -0.11 \pm 0.04$). These results indicate the influence of fluctuations in respiratory rhythm on the blood pressure variability in these data.

For the remaining RES and BPV time series, the coupling is symmetrical, since the average value of the coupling asymmetry indicator $\triangle$MCR(RES|BPV) $= 0.04 \pm 0.01$ and both estimates of the coupling direction indicators are positive: $\gamma_{\mathrm{BPV}} - 1.6\sigma_{\mathrm{BPV}} = 0.09 \pm 0.02$, $\gamma_{\mathrm{RES}} - 1.6\sigma_{\mathrm{RES}} = 0.06 \pm 0.02$. These data are characterized by the interdependent influence of the rhythm of the respiratory system and fluctuations in blood pressure.

For the time series NAV and RES before pain exposure, a unidirectional coupling was found in 65% of the data (18 out of 28) using joint recurrence analysis ($\triangle$MCR(NAV|RES) $= -0.18 \pm 0.05$) and for 61% of data (17 out of 28) using phase dynamics modeling ($\gamma_{\mathrm{RES}} - 1.6\sigma_{\mathrm{RES}} = -0.14 \pm 0.04$, $\gamma_{\mathrm{NAV}} - 1.6\sigma_{\mathrm{NAV}} = 0.16 \pm 0.05$). This coupling is related to the influence of fluctuations in the respiratory rhythm on the neuronal activity variability. For the rest of the analyzed data, the coupling between the NAV and RES time series is symmetric ($\triangle$MCR(NAV|RES) $= 0.05 \pm 0.01$ and $\gamma_{\mathrm{RES}} - 1.6\sigma_{\mathrm{RES}} = 0.12 \pm 0.03$, $\gamma_{\mathrm{NAV}} - 1.6\sigma_{\mathrm{NAV}} = 0.13 \pm 0.03$). In these cases, the rhythms of the nervous and respiratory systems turn out to be interdependent.

During the pain exposure, in a series of data in which phase synchronization was absent, in most cases a unidirectional coupling with the same direction of coupling between the analyzed time series was also revealed as before the exposure, that is, no qualitative change in the coupling direction was detected. The predominant influence of BPV$\rightarrow$NAV was detected for 75% of the analyzed data (12 out of 16), the influence of RES$\rightarrow$BPV was detected for 81% of the data (13 out of 16), the influence of RES$\rightarrow$NAV was characteristic for 63% of the data (10 out of 16) with using joint recurrence analysis and for 69% (11 out of 16), 63% (12 out of 16), 56% (9 out of 16) of the analyzed data using phase dynamics modeling.

Thus, the evaluation of the calculated indicators of the directivity of the coupling between experimentally obtained weakly noisy time series with narrow-band filtering to isolate the components of variability in the intervals of neuronal activity and blood pressure with basic frequencies close to the respiratory rhythm frequency allowed us to identify various variants of the relationships. At the same time, the influence of fluctuations in respiratory rhythm on the variability of neuronal activity and blood pressure and the influence of blood pressure variability on the neural activity of the reticular formation of the medulla oblongata were revealed for a larger number of analyzed data.

The predominant influence of respiratory rhythm on blood pressure variability is consistent with the data described in the papers, which indicate that respiratory rhythm often controls the rhythm of the cardiovascular system [7, 8, 37]. The absence of a pronounced influence of the nervous system in most of the analyzed data may be due to anesthesia, which reduces the influence of pain exposure sensitivity on the respiratory and cardiovascular systems [4, 36].

Conclusion

The aim of the study was to apply two methods of nonlinear dynamics related to modeling the phase dynamics of weakly coupled and weak noise periodic processes and calculating conditional recurrence probabilities of time series to identify the characteristics of the relationship between time series extracted from physiological rhythms.

The analyzed time series corresponded to fluctuations in respiratory rhythm, curves of blood pressure variability, and variability of neuronal activity intervals in the rat medulla oblongata.

Preliminary application of these methods to a well-studied model of two interacting oscillators with known phase synchronization properties to test the stability of the methods to noise confirmed the correct determination of the coupling direction by both methods with weak noise at relatively high coupling coefficients and a decrease in the possibility of detecting the coupling direction using the phase modeling method with increasing noise, but the possibility of correctly determining the coupling direction using analysis of joint recurrences.

The results of using two methods to calculate estimates of the direction of the coupling between experimentally obtained weakly noisy time series with narrowband filtering and with fundamental frequencies close to the respiratory rate turned out to be quite consistent. In most of the analyzed data with a low phase synchronization coefficient, a unidirectional coupling was found in which fluctuations in respiratory rhythm influence the variability of neuronal activity and blood pressure, and blood pressure variability influences the neural activity of the reticular formation of the medulla oblongata.

Appendix

1. Calculation of the unbiased estimate γ_X of the value c_X^2, dispersion estimates $\sigma_{\gamma_X}^2$ for γ_X and noise dispersion estimates $\sigma_{\varepsilon_X}^2$ for the signal x and similar calculations for the signal y are performed according to the formulas given in [32]:

$$\gamma_X = c_X^2 - r_x = c_X^2 - \sum_k n_k^2 \sigma_{X,k}^2, \tag{19}$$

where the estimate $\sigma_{X,k}^2$ of the dispersion coefficients $a_{X,k}$ of the polynomials of the function $F_X(\phi_X, \phi_Y, a_X)$ defined by

$$\sigma_{X,k}^2 = \frac{2\sigma_{\varepsilon_X}^2}{N}\left[1 + 2\sum_{j=1}^{b-1}(1 - j/b)\cos\left[(m_k a_{X,1} + n_k a_{Y,1})j/b\right]\exp\left[-(m_k^2\sigma_{\varepsilon_X}^2 + n_k^2\sigma_{\varepsilon_Y}^2)j/2b\right]\right], \tag{20}$$

where $k = 1, ..., L$, where L is the number of coefficients of the polynomial, $b = \tau/\Delta t$, estimate $\sigma_{\varepsilon_X}^2$ noise dispersion:

$$\sigma_{\varepsilon_X}^2 = \frac{1}{N-1}\sum_{i=1}^{N}\left[[\phi_X(t_i + \tau) - \phi_X(t_i)] - \frac{1}{N}\sum_{i=1}^{N}[\phi_X(t_i + \tau) - \phi_X(t_i)]\right]^2. \tag{21}$$

2. Estimation of the dispersion $\sigma_{\gamma_X}^2$ for the value γ_X:

$$\sigma_{\gamma_X}^2 = \sum_k n_k^4 \sigma_{a_{X,k}^2}^2, \tag{22}$$

if $\gamma_X > 5\sum_k n_k^4 \sigma_{a_{X,k}^2}^2$,

$$\sigma_{\gamma_X}^2 = 0.5\sum_k n_k^4 \sigma_{a_{X,k}^2}^2, \tag{23}$$

if $\gamma_X \leqslant \sum_k n_k^4 \sigma^2_{a^2_{X,k}}$, where

$$\sigma^2_{a^2_{X,k}} = 2\sigma^4_{X,k} + 4[a^2_{X,k} - \sigma^2_{X,k}]\sigma^2_{X,k}, \tag{24}$$

if $a^2_{X,k} - \sigma^2_{X,k} \geqslant 0$,

$$\sigma^2_{a^2_{X,k}} = 2\sigma^4_{X,k}, \tag{25}$$

if $a^2_{X,k} - \sigma^2_{X,k} < 0$.

References

1. Kiselev AR, Mironov SA, Karavaev AS, Kulminskiy DD, Skazkina VV, Borovkova EI, Shvartz VA, Ponomarenko VI, Prokhorov MD. A comprehensive assessment of cardiovascular autonomic control using photoplethysmograms recorded from the earlobe and fingers. Physiol. Meas. 2016;37(4):580–595. DOI: 10.1088/0967-3334/37/4/580.
2. Khorev VS, Ishbulatov JM, Lapsheva EE, Kiselev AR, Gridnev VI, Bezruchko BP, Butenko AA, Ponomarenko VI, Karavaev AS. Diagnostics of directional coupling between blood circulation regulation loops using analysis of time series of mathematical model of human cardiovascular system. Information and Control Systems. 2018;1:42–48. DOI: 10.15217/issn1684-8853.2018.1.42.
3. Rosenblum MG, Cimponeriu L, Bezerianos A, Patzak A, Mrowka R. Identification of coupling direction: application to cardiorespiratory interaction. Phys. Rev. E. 2002;65(4):041909. DOI: 10.1103/PhysRevE.65.041909.
4. Shiogai Y, Stefanovska A, McClintock PVE. Nonlinear dynamics of cardiovascular ageing. Phys. Rep. 2010;488(2–3):51–110. DOI: 10.1016/j.physrep.2009.12.003.
5. Rosenblum M.G., Pikovsky A.S. Detecting direction of coupling in interacting oscillators. Phys. Rev. E. 2001;64(4):045202. DOI: 10.1103/PhysRevE.64.045202.
6. Bahraminasab A, Ghasemi F, Stefanovska A, McClintock PV, Kantz H. Direction of coupling from phases of interacting oscillators: a permutation information approach. Phys. Rev. Lett. 2008;100(8):084101. DOI: 10.1103/PhysRevLett.100.084101.
7. Mrowka R, Cimponeriu L, Patzak A, Rosenblum MG. Directionality of coupling of physiological subsystems: age-related changes of cardiorespiratory interaction during different sleep stages in babies. Am. J. Physiol. Regul. Integr. Comp. Physiol. 2003;285(6):R1395–R1401. DOI: 10.1152/ajpregu.00373.2003.
8. Ocon AJ, Medow MS, Taneja I, Stewart JM. Respiration drives phase synchronization between blood pressure and RR interval following loss of cardiovagal baroreflex during vasovagal syncope. Am. J. Physiol. Heart Circ. Physiol. 2011;300(2):H527–H540. DOI: 10.1152/ajpheart.00257.2010.
9. Dick TE, Hsieh YH, Dhingra RR, Baekey DM, Galán RF, Wehrwein E, Morris KF. Cardiorespiratory coupling: common rhythms in cardiac, sympathetic, and respiratory activities. Prog Brain Res. 2014;209:191–205. DOI: 10.1016/B978-0-444-63274-6.00010-2.
10. Hlavackova-Schindler K, Palus M, Vejmelka M, Bhattacharya J. Causality detection based on information-theoretic approaches in time series analysis. Phys. Rep. 2007;441(1):1–46. DOI: 10.1016/j.physrep.2006.12.004.
11. Smirnov DA. Quantifying causal couplings via dynamical effects: A unifying perspective. Phys. Rev. E. 2014;90(6):062921. DOI: 10.1103/PhysRevE.90.062921.
12. Faes L, Nollo G, Chon K. Assessment of Granger causality by nonlinear model identification: application to short-term cardiovascular variability. Ann. Biomed. Eng. 2008;36:381–395. DOI: 10.1007/s10439-008-9441-z.

13. Schreiber T. Measuring information transfer. Phys. Rev. Lett. 2000;85(2):461–464. DOI: 10.1103/PhysRevLett.85.461.
14. Baccala LA, Sameshima K. Partial directed coherence: A new concept in neural structure determination. Biol. Cybern. 2001;84(6):463–474. DOI: 10.1007/PL00007990.
15. Navrotskaya EV, Smirnov DA, Bezruchko BP. Reconstruction of the structure of connections in an ensemble of oscillators from recordings of oscillations through modeling of phase dynamics. Izvestiya VUZ. Applied Nonlinear Dynamics. 2019;27(1):41–52. DOI: 10.18500/0869-6632-2019-27-1-41-52.
16. Sidak EV, Smirnov DA, Bezruchko BP. Estimation of the time delay of coupling between oscillators from time realizations of oscillation phases for different properties of phase dynamics. Journal of Communications Technology and Electronics. 2017;62(3):241–250. DOI: 10.1134/S1064226917030196.
17. Romano MC, Thiel M, Kurths J, Grebogi C. Estimation of the direction of the coupling by conditional probabilities of recurrence. Phys. Rev. E. 2007;76(3):036211. DOI: 10.1103/PhysRevE.76.036211.
18. Marwan N, Zou Y, Wessel N, Riedl M, Kurths J. Estimating coupling directions in the cardiorespiratory system using recurrence properties. Philos. Trans. A Math. Phys. Eng. Sci. 2013;371:20110624. DOI: 10.1098/rsta.2011.0624.
19. Pereda E, Quiroga RQ, Bhattacharya J. Nonlinear multivariate analysis of neurophysiological signals. Prog. Neurobiol. 2005;77(1–2):1–37. DOI: 10.1016/j.pneurobio.2005.10.003.
20. Sysoeva MV, Sitnikova E, Sysoev IV, Bezruchko BP, van Luijtelaar G. Application of adaptive nonlinear Granger causality: Disclosing network changes before and after absence seizure onset in a genetic rat model. J. Neurosci. Methods. 2014;226:33–41. DOI: 10.1016/j.jneumeth.2014.01.028.
21. Sysoeva MV, Kuznetsova GD, Sysoev IV. The modeling of rat EEG signals in absence epilepsy in the analysis of brain connectivity. Biophysics. 2016;61(4):661–669. DOI: 10.1134/S0006350916040230.
22. Smirnov DA, Barnikol UB, Barnikol TT, Bezruchko BP, Hauptmann C, Buhrle C, Maarouf M, Sturm V, Freund H-J, Tass PA. The generation of parkinsonian tremor as revealed by directional coupling analysis. Europhysics Letters. 2008;83(2):20003. DOI: 10.1209/0295-5075/83/20003.
23. Sysoeva MV, Sysoev IV. Mathematical modeling of encephalogram dynamics during epileptic seizure. Tech. Phys. Lett. 2012;38(2):151–154. DOI: 10.1134/S1063785012020137.
24. Mokhov II, Smirnov DA. El Nino Southern Oscillation drives North Atlantic Oscillation as revealed with nonlinear techniques from climatic indices. Geophys. Res. Lett. 2006;33(3):L03708. DOI: 10.1029/2005GL024557.
25. Mokhov II, Smirnov DA, Nakonechny PI, Kozlenko SS, Kurths J. Relationship between El-Niño/Southern Oscillation and the Indian monsoon. Izvestiya, Atmospheric and Oceanic Physics. 2012;48(1):47–56. DOI: 10.1134/S0001433812010082.
26. Dick OE. Synchronization analysis of time series obtained from anesthetized rats during painful action Izvestiya VUZ Applied Nonlinear Dynamics. 2024;32(2):209–222. DOI: 10.18500/0869-6632-003093.
27. Marwan N, Romano MC, Thiel M, Kurths J. Recurrence plots for the analysis of complex systems. Phys. Rep. 2007;438(5–6):237–329. DOI: 10.1016/j.physrep.2006.11.001.
28. Takens F. Detecting strange attractors in turbulence. In: Rand D, Young LS, editors. Dynamical Systems and Turbulence, Warwick 1980. Lecture Notes in Mathematics. Vol. 898. Berlin: Springer; 1981. P. 366–381. DOI: 10.1007/BFb0091924.
29. Kennel MB, Brown R, Abarbanel HD. Determining embedding dimension for phase-space reconstruction using a geometrical construction. Phys. Rev. A. 1992;45(6):3403–3411.

DOI: 10.1103/physreva.45.3403.
30. Fraser AM, Swinney HL. Independent coordinates for strange attractors from mutual information Phys. Rev. A. 1986;33(2):1134–1140. DOI: 10.1103/physreva.33.1134.
31. Kurths J, Romano MC, Thiel M, Osipov GV, Ivanchenko MV, Kiss IZ, Hudson JL. Synchronization analysis of coupled noncoherent oscillators. Nonlinear Dyn. 2006;44: 135–149. DOI: 10.1007/s11071-006-1957-x.
32. Smirnov DA, Bezruchko BP. Estimation of interaction strength and direction from short and noisy time series. Phys. Rev. E. 2003;68:046209. DOI: 10.1103/PhysRevE.68.046209.
33. Smirnov DA. Characterization of weak coupling between self-oscillation systems from short time series: Technique and applications. Journal of Communications Technology and Electronics. 2006;51(5):534–544. DOI: 10.1134/S106422690605007X.
34. Smirnov DA, Bodrov MB, Bezruchko BP. Estimation of coupling between oscillations from time series via phase dynamics modeling: limits of method. Izvestiya VUZ Applied Nonlinear Dynamics. 2004;12(6):79–92. DOI: 10.18500/0869-6632-2004-12-6-79-92.
35. Daubechies I, Lu J, Wu HT. Synchrosqueezed wavelet transforms: An empirical mode decomposition-like tool. Appl. Comput. Harmon. Anal. 2011;30(2):243–261. DOI: 10.1016/j.acha.2010.08.002.
36. Thiel M, Romano MC, Kurths J, Rolfs M, Kliegl R. Generating surrogates from recurrences. Philos. Trans. A Math. Phys. Eng. Sci. 2008;366(1865):545–557. DOI: 10.1098/rsta.2007.2109.
37. Stefanovska A, Haken H, McClintock PVE, Hozic M, Bajrovic F, Ribaric S. Reversible transitions between synchronization states of the cardiorespiratory system. Phys Rev Lett. 2000;85:4831–4834. DOI: 10.1103/PhysRevLett.85.4831.
38. Ponomarenko VI, Prokhorov MD, Bespyatov AB, Bodrov MB, Gridnev VI. Deriving main rhythms of the human cardiovascular system from the heartbeat time series and detecting their synchronization. Chaos, Solitons and Fractals. 2005;23(4):1429–1438. DOI: 10.1016/j.chaos.2004.06.041.
39. Dick OE, Glazov AL. Revealing the coupling directionality and synchronization between time series from physiological data by analysis of joint recurrences. Chaos, Solitons and Fractals. 2023;173:113768. DOI: 10.1016/j.chaos.2023.113768.